Journal of Thermal Analysis, Vol. 54 (1998) 437-465

ABOUT COMPLEX HEAT CAPACITIES AND TEMPERATURE-MODULATED CALORIMETRY

H. Baur and B. Wunderlich*

Department of Chemistry, The University of Tennessee, Knoxville, TN 37996-1600, and the Chemical and Analytical Sciences Division, Oak Ridge National Laboratory, Oak Ridge, TN 37831-6197, USA

Abstract

With increasing use of temperature-modulated calorimetry, TMC, it is has been proposed to use a complex heat capacity for the description of the response of samples to periodic temperature changes. In this article the ramifications of this approach are discussed on the basis of irreversible thermodynamics. Experimental results are summarized which describe heat capacities of liquids and solids, as well as TMC during transitions. It is concluded that the complex heat capacity is of limited value. Solids and liquids have no dissipative (imaginary) contributions. In the glass transition, the thermal response is nonlinear, so that a detailed kinetic model (in real notation) is more advantageous to describe the heat capacity. The crystallization is often so far from equilibrium that it is not modulated. During melting and chemical reactions the heat flow is frequently so large, that steady state is lost and complex heat capacity is of questionable value, even if modulation is accomplished.

Keywords: complex heat capacity, heat capacity, irreversible thermodynamics, temperature-modulated calorimetry

Introduction

In general, one can represent a complex number $z=a+ib$[a], with $i=\sqrt{-1}$, as:

$$z = |z|e^{i\theta} = |z|(\cos\theta + i\sin\theta), \text{ with} \quad (1a)$$

* Sonnenwendstr. 41. D-67098 Bad Dürkheim, Germany

[a] Note that a and b are real numbers. The complex numbers $z=(x,y)$ have the following addition and multiplications rules: $(a,b)+(c,d)=(a+c,b+d)$ and $(a,b)\times(c,d)=(ac-bd,ad+bc)$. The real numbers a and b are the real and imaginary parts of the complex number (a,b). The terms real and imaginary are historical accidents since both a and b are real numbers, and complex numbers are often useful to describe real phenomena. It is easy to see from $(0,1)\times(0,1)$ that $i\equiv\sqrt{-1}$.

1418–2874/98/ $ 5.00

Akadémiai Kiadó, Budapest
Kluwer Academic Publishers, Dordrecht

$$|z| = \sqrt{a^2 + b^2};\ \cos\theta = \frac{a}{|z|} \text{ and } \sin\theta = \frac{b}{|z|}. \quad (1b)$$

Any periodic process with an angular frequency of $\omega=2\pi\nu$, where ν is the oscillation frequency in Hz (s^{-1}), can therefore be depicted by a uniform motion tracing a circle in the plane mapping the complex numbers:

$$Ae^{i\omega t} = A(\cos\omega t + i\sin\omega t).$$

For the description of periodic changes or a Fourier analysis of complicated processes the introduction of complex quantities is convenient and lucid. Naturally, it can bring no new physical insight over the representation in real numbers.

The so-called linear response theory makes extensive use of the possibility of complex formulations in its treatment of dissipative systems [1]. The response functions appear as complex quantities $\chi'+i\chi''$ with the real component χ' representing the reactive part, and the imaginary component $\chi''\geq 0$, the dissipative part. Preconditions for linearity are fixed internal equilibrium states as reference, and sufficiently small deviations from these states. The question whether a complex representation is suitable for heat capacity is to be investigated in this paper.

The similarity of the description of temperature-modulated DSC (TMDSC) and dynamic mechanical analysis (DMA) and also dielectric thermal analysis (DETA) has brought up this question whether a complex heat capacity and the application of linear response theory would be of use in TMDSC [2]. Analysis of the instrumentation [3] has established that one must determine two phase lags relative to the reference frequency ω. First, the effect that represents the calorimeter response to the oscillating heater temperature. Second, the sample response. In case of a sample that has no slowly responding modes of motion, as in heat capacities of solids and liquids, there should be no lag due to the sample response. Typically, the response of molecular modes of motion to heat flow are in the picosecond range (10^{-12} s) [4]. The lag measured [5] is then entirely due to the thermal conductivity of the calorimeter. Note, that one of the basic conditions of DSC is that there be a negligible temperature gradient within the sample so that the effect due to the thermal conductivity of the sample is negligible [6]. The apparent heat capacity in the glass transition region, in contrast, is time dependent [7] and there should be an additional phase lag of the heat flow relative to the amplitude of the sample temperature [8]. Only this latter phase lag is to be discussed in the present paper.

In TMDSC the heat capacity is calculated from the modulation amplitude or phase lag of the heat flow responding to the sample-temperature modulation. The complex representation of this calculation for fast responding systems is well understood [9]. It is based entirely on the thermal conductivity of the path between heater and sample and reference calorimeters. Finally, it should be remarked that

a complex heat capacity has proven useful in the interpretation of thermal conductivity of gases with slowly responding internal degrees of freedom for the understanding of dispersion and absorption of high-frequency sound waves [10].

Formulation of the complex heat capacity

Equilibrium and nonequilibrium heat capacities

In the following, only homogeneous systems with constant mass will be treated. The dissipative effects are caused in such homogeneous systems by disturbance of the equilibrium of the internal molecular degrees of freedom. The determining, actual internal degrees of freedom often do not appear in the linear response theory because linearity and relation to the fixed internal equilibrium permit their elimination. In order to better understand the processes it is, however, useful to explicitly consider the variables of the molecular degrees of freedom. In the following a homogeneous system with a single relevant molecular degree of freedom will be considered. This degree of freedom will be assigned the (macroscopic) internal variable ζ. In the case of a glass transition, ζ could, for example, describe the concentration of the microscopic vacancies (number of holes, N_h). In the past we have used the hole theory as applied by Hiray and Eyring [11] for the approximate description of the glass transition [7, 12].

The starting point for the description of the system considered is the Gibbs fundamental equation:

$$g(T,p,\zeta) = h(T,p,\zeta) - Ts(T,p,\zeta), \tag{2}$$

written in Eq. (2) as the specific free enthalpy g as function of the mutually independent variables temperature, T, hydrostatic pressure, p, and internal variable, ζ. The specific entropy, s, and the specific enthalpy, h, of the system are:

$$s = -\left(\frac{\partial g}{\partial T}\right)_{p,\zeta} \; ; \quad h = g - T\left(\frac{\partial g}{\partial T}\right)_{p,\zeta} .$$

Dissipative processes are non-equilibrium processes where the independent variables $T(t)$, $p(t)$, and $\zeta(t)$ are directly dependent functions of time, t. In homogeneous systems, the changes with time, $\dot{T} \equiv dT/dt$ and $\dot{p} \equiv dp/dt$, are given by the external perturbation. The change of the internal variable with time, $\dot{\zeta}$ may be given by a dynamic law of the form:

$$\dot{\zeta} = La \quad \text{with} \quad L \geq 0 \tag{3}$$

where $a(T,p,\zeta)$ is the so-called affinity, which for the internal variable has the meaning of a driving force, and L is the so-called phenomenological coefficient (for example [13]) or coupling factor. The affinity is given by:

$$a \equiv -\left(\frac{\partial g}{\partial \zeta}\right)_{T,p} = T\sigma_{T,p} - \eta_{T,p} \tag{4}$$

where $\sigma_{T,p}$ and $\eta_{T,p}$ are the partial specific entropy and enthalpy, respectively, relative to the internal degree of freedom:

$$\sigma_{T,p} \equiv \left(\frac{\partial s}{\partial \zeta}\right)_{T,p} \quad \text{and} \quad \eta_{T,p} \equiv \left(\frac{\partial h}{\partial \zeta}\right)_{T,p} . \tag{5}$$

At internal equilibrium the affinity goes to zero. An internal state of equilibrium, indicated by the superscript 'e', is thus given by:

$$a^e = 0 \quad \text{resp.} \quad T\sigma^e_{T,p} = \eta^e_{T,p} . \tag{6}$$

Equation (6) fixes one of the independent variables as function of the other. One can, thus, determine the equilibrium value of the internal variable with help of Eq. (6):

$$\zeta = \zeta^e(T,p).$$

During internal equilibrium, ζ remains variable, but it is not an independent variable. For a change of the affinity as a function of the independent variables one gets:

$$\mathrm{d}a = \left(\frac{\partial a}{\partial T}\right)_{p,\zeta} \mathrm{d}T + \left(\frac{\partial a}{\partial p}\right)_{T,\zeta} \mathrm{d}p + \left(\frac{\partial a}{\partial \zeta}\right)_{T,p} \mathrm{d}\zeta. \tag{7}$$

At internal equilibrium (da=0), the following holds (Eqs (4) and (5)):

$$\left(\frac{\partial a}{\partial T}\right)^e_{p,\zeta} = -\left(\frac{\partial^2 g}{\partial T \partial \zeta}\right)^e = -\left(\frac{\partial^2 g}{\partial \zeta \partial T}\right)^e = \sigma^e_{T,p} \tag{8}$$

$$\left(\frac{\partial a}{\partial \zeta}\right)^e_{T,p} = -\left(\frac{\partial^2 g}{\partial \zeta^2}\right)^e_{T,p}$$

and the change of the internal variable with temperature at constant pressure and at equilibrium is given by insertion into Eq. (7) as:

$$\left(\frac{\partial \zeta}{\partial T}\right)^e_p = \frac{\sigma^e_{T,p}}{\left(\frac{\partial^2 g}{\partial \zeta^2}\right)^e_{T,p}} . \tag{9}$$

The product $L(\partial^2 g/\partial\zeta^2)_{T,p}$ has the dimension of a reciprocal time if the internal variable is dimensionless (for example, if ζ represents a mole fraction). In a simple relaxation experiment, under the condition that T and p are constant, one can show that the Debye relaxation time of the system is:

$$\tau^{e}_{T,p}(T,p) = \frac{1}{L\left(\frac{\partial^2 g}{\partial\zeta^2}\right)^{e}_{T,p}} \geq 0. \tag{10}$$

Analogously, one can also introduce the relaxation time:

$$\tau_{T,p}(T,p,\zeta) = \frac{1}{L\left(\frac{\partial^2 g}{\partial\zeta^2}\right)_{T,p}} \tag{11}$$

which, in contrast to the Debye relaxation time, depends also on ζ. With help of Eq. (10) one can then also write instead of Eq. (9):

$$\left(\frac{\partial\zeta}{\partial T}\right)^{e}_{p} = L\tau^{e}_{T,p}\sigma^{e}_{T,p}. \tag{12}$$

The change of the entropy with respect to the independent variables is given by:

$$ds = \left(\frac{\partial s}{\partial T}\right)_{p,\zeta} dT + \left(\frac{\partial s}{\partial p}\right)_{T,\zeta} dp + \left(\frac{\partial s}{\partial\zeta}\right)_{T,p} d\zeta. \tag{13}$$

The specific heat capacity at constant pressure can then be derived from:

$$c_p = T\left(\frac{ds}{dT}\right)_p = T\left(\frac{\partial s}{\partial T}\right)_{p,\zeta} + T\sigma_{I,p}\left(\frac{d\zeta}{dT}\right)_p \tag{14}$$

where:

$$c_{p,\zeta} = T\left(\frac{ds}{dT}\right)_{p,\zeta} \tag{15}$$

is the specific heat capacity of the so-called arrested equilibrium (ζ=constant). This specific heat capacity is measured when the change in temperature occurs sufficiently fast that the inner degree of freedom cannot follow this change ($\zeta << T$) or if the internal degree of freedom is frozen (ζ=0, because $L \to 0$; see below). For the example of the glass transition this is the specific heat capacity of

the solid, c_p^o (Sect. Discussions). In internal equilibrium, one measures the specific heat capacity as (Eqs (14) and (15)):

$$c_p^e = c_{p,\zeta^e} + \Delta^e c_p \tag{16a}$$

where $\Delta^e c_p$ is the specific-heat-capacity contribution of the internal degree of freedom to the internal equilibrium, which can be expressed with Eq. (12) as:

$$\Delta^e c_p = TL\tau_{T,p}^e(\sigma_{T,p}^e)^2 \geq 0. \tag{16b}$$

Outside of the equilibrium, i.e. in non-equilibrium, T and ζ are variables that are independent of each other. With p=constant one must then set:

$$\left(\frac{d\zeta}{dT}\right)_p = \frac{\dot{\zeta}}{\dot{T}}. \tag{17}$$

Under conditions of non-equilibrium, one measures:

$$c_p = c_{p,\zeta} + \Delta c_p, \text{ with} \tag{18a}$$

$$\Delta c_p = T\sigma_{T,p}\frac{\dot{\zeta}}{\dot{T}} \tag{18b}$$

where Δc_p is the contribution of the internal degree of freedom to the specific heat capacity under conditions of non-equilibrium.

Complex specific heat capacity

For the change of the affinity with respect to time at constant pressure it follows from Eqs (7), (8), and (11) that:

$$\dot{a} = \left(\frac{\partial a}{\partial T}\right)_{p,\zeta}\dot{T} - \frac{1}{L\tau_{T,p}}\dot{\zeta}.$$

If, furthermore, the coupling factor L in Eq. (3) is constant, it follows from Eq. (3) that:

$$\ddot{\zeta} - L\dot{a}.$$

Both equations together yield, at constant pressure, the non-linear differential equation for the determination of the internal variable $\zeta(t)$ as function of time, t:

$$\ddot{\zeta} + \frac{1}{\tau_{T,p}}\dot{\zeta} - L\left(\frac{\partial a}{\partial T}\right)_{p,\zeta}\dot{T} \tag{19}$$

where $\dot{T}$ is given through the external perturbation of the system. The right side of Eq. (19) expresses also the external force which acts on the internal, molecular degree of freedom. As first integral of Eq. (19) one finds:

$$\dot{\zeta}(t) = e^{-\lambda_{T,p}(t)}\left[\dot{\zeta}(0) + L\int_0^t \left(\frac{\partial a}{\partial T}\right)_{p,\zeta} e^{\lambda_{T,p}(t')}\dot{T}(t')dt'\right] \tag{20a}$$

with the dimensionless, relative time variable:

$$\lambda_{1,p}(t) = \int_0^t \frac{dt'}{\tau_{T,p}}. \tag{20b}$$

If one assumes the internal equilibrium 'e' as initial state, $\dot{\zeta}(0)$ becomes zero. Taking this internal equilibrium as reference state and assuming further that the deviations ΔT from T^e are small, one can relate all coefficients in Eqs (19) and (20) to this equilibrium state and consider them constant. Equation (19) becomes then a linear equation and the first integral is, with the use of Eq. (8):

$$\lambda_{T,p}(t) = -\frac{t}{\tau^e_{T,p}}, \text{ and} \tag{21a}$$

$$\dot{\zeta}(t) = L\sigma^e_{T,p}e^{-t/\tau^e_{T,p}}\int_0^t e^{t'/\tau^e_{T,p}}\dot{T}(t')dt'. \tag{21b}$$

If the disturbance $\dot{T}$ of the system is periodic with a frequency of $\nu(\omega=2\pi\nu)$, one finds in complex notation with a modulation amplitude A_T:

$$T(t) = T^e + A_T e^{i\omega t}, \text{ and} \tag{22a}$$

$$\dot{T}(t) = i\omega A_T e^{i\omega t} = i\omega[T(t) - T^e]. \tag{22b}$$

Because $i=e^{-i\pi/2}$, $\dot{T}$ is phase shifted by 90° relative to $T(t)$. The zero of time is to be chosen at $-\infty$ for a strictly periodic perturbation. It results then from Eqs (21) and (22) that:

$$\dot{\zeta}(t) = L\sigma^e_{\nu,p}e^{-t/\tau^e_{T,p}}i\omega A_T\int_{-\infty}^t e^{(i\omega+1/\tau^e_{T,p})t'}dt', \quad \text{i.e.} \tag{23}$$

$$\dot{\zeta}(t) = L\tau^e_{T,p}\sigma^e_{T,p}\frac{i\omega A_T}{1 + i\omega\tau^e_{T,p}}e^{i\omega t}.$$

Finally, a second integration gives the complex solution:

$$\zeta(t) = \zeta^e + L\tau^e_{T,p}\sigma^e_{T,p}\frac{A_T}{1 + i\omega\tau^e_{T,p}}e^{i\omega t}, \tag{24a}$$

or with Eqs (12) and (22a):

$$\zeta(t) = \zeta^e + \left(\frac{d\zeta}{dT}\right)^e_p \frac{T(t) - T^e}{1 + i\omega\tau^e_{T,p}}. \tag{24b}$$

The internal variable changes also periodically. There exists, however, a phase shift γ between the perturbation $T(t)-T^e$ and the reaction $\zeta(t)-\zeta^e$ because (Eq. (1)):

$$\frac{1}{1 + i\omega\tau^e_{T,p}} = \frac{1}{\sqrt{1 + \omega^2(\tau^e_{T,p})^2}}e^{-i\gamma};\ \tan\gamma = \omega\tau^e_{T,p}.$$

In the range $\omega\tau^e_{T,p}<<1$, the internal variable $\zeta(t)$ follows the external perturbation practically instantaneously with $\gamma=0$. This corresponds to a quasi-static perturbation without dissipative effect. In the range $\omega\tau^e_{T,p}>>1$, in contrast, $\zeta(t)-\zeta^e$ lags with $\gamma\approx 90^\circ$ behind the external perturbation. The amplitude of $\zeta(t)-\zeta^e$ decreases continually with increasing ω until in the limit $\omega \to \infty$, $\zeta(t)-\zeta^e$=constant. The latter describes the case of an arrested equilibrium.

The ratio $\dot{\zeta}/\dot{T}$ can be expressed with Eqs (22), (23) and (12) as:

$$\frac{\dot{\zeta}}{\dot{T}} = L\tau^e_{T,p}\sigma^e_{T,p}\frac{1}{1 + i\omega\tau^e_{T,p}} = \left(\frac{d\zeta}{dT}\right)^e_p \frac{1}{1 + i\omega\tau^e_{T,p}} \tag{25}$$

Insertion of Eq. (25) into Eq. (18) yields with Eq. (16) the complex, frequency-dependent specific heat capacity:

$$c_p(\omega) = c_{p,\zeta^e} + \frac{\Delta^e c_p}{1 + i\omega\tau^e_{T,p}}. \tag{26}$$

To divide $c_p(\omega)$ into a reactive part c'_p and a dissipative part c''_p, one must use the following equation to make the dissipative part, c''_p, positive (since $\Delta^e c_p \geq 0$):

$$c_p(\omega) = c'_p(\omega) - ic''_p(\omega). \tag{27}$$

The real quantities can then be derived from Eq. (26):

$$c'_p(\omega) = c_{p,\zeta^e} + \frac{\Delta^e c_p}{1 + \omega^2(\tau^e_{T,p})^2} \tag{28}$$

$$c_p''(\omega) = \frac{\omega\tau^e_{T,p}\Delta^e c_p}{1+\omega^2(\tau^e_{T,p})^2}. \tag{29}$$

Instead of Eq. (28) one can also write, by making use of Eq. (16a):

$$c_p'(\omega) = c_p^e - \frac{\omega^2(\tau^e_{T,p})^2\Delta^e c_p}{1+\omega^2(\tau^e_{T,p})^2}. \tag{30}$$

The reactive and dissipative parts are not independent of each other. From Eqs (28) to (30) it follows that:

$$c_p(\omega) = c^e_{p,\zeta} + \frac{1}{\omega\tau^e_{T,p}} c_p''(\omega) \quad \text{and} \tag{31a}$$

$$c_p'(\omega) = c_p^e - \omega\tau^e_{T,p} c_p''(\omega). \tag{31b}$$

The reactive part c_p' of the complex specific heat capacity is the dynamic analog of the heat capacity of the equilibrium. Accordingly, the limiting cases of the internal and arrested equilibrium are:

$$\omega\tau^e_{T,p} << 1; \quad c_p(\omega) = c_p'(\omega) = c_p^e, \quad \text{and} \tag{32a}$$

$$\omega\tau^e_{T,p} >> 1; \quad c_p(\omega) = c_p'(\omega) = c_{p,\zeta^e}. \tag{32b}$$

The internal degree of freedom contributes at sufficiently low frequencies the total equilibrium contribution, $\Delta^e c_p$, to the specific heat capacity. With increasing frequency this contribution decreases, and it disappears at very high frequencies.

The dissipative part, c_p'', has naturally no analog in the equilibrium thermodynamics. In the limiting cases of Eqs (32) one derives from Eq. (29):

$$\omega\tau^e_{T,p} << 1; \quad c_p''(\omega) = \omega\tau^e_{T,p}\Delta^e c_p, \quad \text{and} \tag{33a}$$

$$\omega\tau^e_{T,p} >> 1; \quad c_p''(\omega) = \frac{\Delta^e c_p}{\omega\tau^e_{T,p}}. \tag{33b}$$

so that the dissipative part disappears in internal equilibrium ($\omega \to 0$) as well as in arrested equilibrium ($\omega \to \infty$).

The dissipative heat capacity $c_p''(\omega)$ is a measure of the entropy produced in non-equilibrium per half-period of the oscillation $T(t)-T^e$. Assuming a dynamic law of the form of Eq. (3), one can write the produced entropy per unit time and mass within the system [13]:

$$\frac{d_i s}{dt} = \frac{1}{LT}\dot{\zeta}^*(t)\dot{\zeta}(t) \geq 0 \tag{34}$$

where ζ^* is the conjugated complex quantity of ζ (which is obtained on replacing i by $-i$ in Eq. (23)). It follows from Eq. (23) that:

$$\frac{d_i s}{dt} = \frac{1}{T_e}(\Delta T \sigma^e_{T,p})^2 \frac{\omega^2(\tau^e_{T,p})^2}{1+\omega^2(\tau^e_{T,p})^2}.$$

The entropy produced per half-period of the oscillation is:

$$\Delta_i s \equiv \int_{\pi n/\omega}^{\pi(n+1)/\omega} \frac{d_i s}{dt} dt = \pi \left(\frac{A_T}{T^e}\right)^2 \frac{\omega \tau^e_{T,p} \Delta^e c_p}{1+\omega^2(\tau^e_{T,p})^2} = \pi \left(\frac{A_T}{T^e}\right)^2 c''_p . \quad (35)$$

Also, one can write:

$$c''_p(\omega) = \frac{1}{\pi}\left(\frac{T^e}{A_T}\right)^2 \Delta_i s. \quad (36)$$

Equation (36) is analogous to the mechanics of linear dissipative systems. For the loss modulus k''_T of the complex bulk modulus, $k_T(\omega)$ one obtains, for example, with a volume modulation A_v:

$$k''_T(\omega) = \frac{v^e}{\pi (A_v)^2} T^e \Delta_i s,$$

where v is the specific volume of the system.

In Fig. 1 plots versus $\ln(\omega\tau^e_{T,p})$ are shown for the reactive heat capacity c'_p according to Eq. (28) and the dissipative heat capacity c''_p according to Eq. (29). The function $c''_p(\omega)$ reaches a maximum at the frequency $\omega = 1/\tau^e_{T,p}$. For perturbation frequencies $\omega \ll 1/\tau^e_{T,p}$, the dissipative part can be practically neglected and it can be assumed that $c_p(\omega) - c'_p - c^e_p$ (Eq. (32a)).

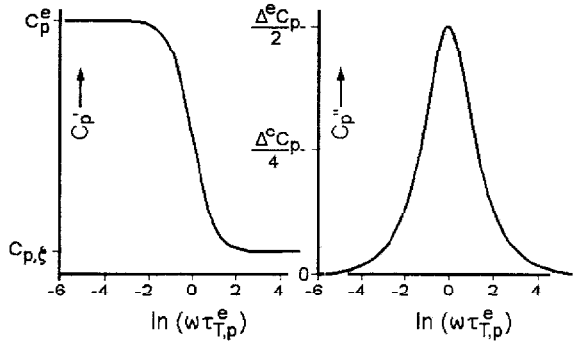

Fig. 1 Reactive part of the complex heat capacity, c'_p as given in Eq. (28) and dissipative part, c''_p as given in Eq. (29) as function of $\ln(\omega\tau^e_{T,p})$. The external perturbation frequency is ω, the Debye relaxation time of the initial state is $\tau^e_{T,p}$

Limits of the linear response theory

Addition of a constant (underlying) heating or cooling rate $\langle\dot{T}\rangle$[b] to the small temperature oscillations given by Eq. (22) causes a continuous displacement of the reference state assumed above. The rate of change of the temperature is then:

$$\dot{T} = \langle\dot{T}\rangle - \omega A_T \sin\omega t. \tag{37}$$

With $\langle\dot{T}\rangle \neq 0$ the reference state is not an internal equilibrium state any more and Eq. (19) remains a non-linear differential equation. The basic precondition of the linear response theory is now not any more fulfilled, i.e. the derivations following Eq. (20) do not hold. With a constant coupling factor L, a linearization of Eq. (19) is only possible under the following two conditions:

1) $(\partial a/\partial T)_{p,\zeta}$ must be practically constant with respect to a change of T and ζ. The constancy with T is frequently acceptable. It requires that $\sigma_{T,p}$ and $\eta_{T,p}$ are approximately independent of temperature. According to Eq. (4) one obtains then:

$$\left(\frac{\partial a}{\partial T}\right)_{p,\zeta} = \sigma_{T,p}\,. \tag{38}$$

This corresponds, even in non-equilibrium, to an interchangeability of the differentiations according to Eq. (8). It remains the dependence of $\sigma_{T,p}$ on ζ. The entropy depends, however, most often logarithmically on ζ. An approximate linear dependence can therefore only be assumed over a very limited range of ζ.

2) $\tau_{T,p}$ must be practically constant with respect to a change of T and ζ. It follows from Eqs (2), (5) and (11) that:

$$\frac{1}{\tau_{T,p}} = L\left[\left(\frac{\partial \eta_{T,p}}{\partial \zeta}\right)_{T,p} - T\left(\frac{\partial \sigma_{T,p}}{\partial \zeta}\right)_{T,p}\right].$$

If the coefficients $(\partial\eta_{T,p}/\partial\zeta)_{T,p}$ and $(\partial\sigma_{T,p}/\partial\zeta)_{T,p}$ are independent of temperature (an often possible assumption) there remains still a hyperbolic dependence of $\tau_{T,p}$ on T. With respect to a change in temperature, $\tau_{T,p}$ is only constant if $(\partial\sigma_{T,p}/\partial\zeta)_{T,p}$ and $(\partial^2 s_{T,p}/\partial\zeta^2)_{T,p}$ are very small. With respect to a change of the internal variable $\tau_{T,p}$ is constant, if the free enthalpy can be represented in a quadratic form:

$$g = g^e + g_1(\zeta - \zeta^e) + g_2(\zeta - \zeta^e)^2.$$

[b] Common usage in temperature-modulated calorimetry is to write $\langle q\rangle$ for the underlying heating rate, where the average $\langle\ \rangle$ is taken over one modulation period, so that the change due to the oscillation averages to zero. In order not to cause confusion, we use in this paper q exclusively to designate heat and do not abbreviate $\dot{T}$.

In the close vicinity of ζ^e, such expansion with $|\zeta-\zeta^e|<<|\zeta^e|$ is often possible. Over larger ranges this expansion is, however, again prevented by the logarithmic dependence of s on ζ. In addition, a quadratic form of the enthalpy $h(\zeta)$ is to be expected only in cases of simple formulations of intermolecular interactions ('simple mixtures' in the Guggenheim sense [14]).

For the glass transition, and more general for any transition from an internal equilibrium to an arrested equilibrium, L can not be considered to be a constant. For a system in an arrested equilibrium relative to the internal variable ζ, $\dot{\zeta}=0$ holds. According to Eq. (3) $\dot{\zeta}$ disappears, however, not because $a=0$ (internal equilibrium), but because $L \rightarrow 0$. For the glass transition, for example, $1/L$ is related to the viscosity of the liquid [36], which changes from small values for the internal equilibrium of the liquid to very high values in the glassy solid ($>10^{13}$ Pa s). The coupling factor must in these cases be of necessity a function of the variables that are independent of each other in non-equilibrium $L=L(T,p,\zeta)$. The differential equation Eq. (19) retains under these conditions the same form only, if the relaxation time $\tau_{T,p}$ is replaced by an effective τ:

$$\frac{1}{\tau_{\text{eff}}}=\frac{1}{\tau_{T,p}}-\left(\frac{\partial \ln L}{\partial T}\right)_{p,\zeta}\dot{T}-\left(\frac{\partial \ln L}{\partial \zeta}\right)_{T,p}\dot{\zeta}. \tag{39}$$

The effective relaxation time of a freezing process depends, thus, not only on the variables T and ζ, but also on their rates $\dot{T}$ and $\dot{\zeta}$:

$$\tau_{\text{eff}}=\tau_{\text{eff}}(T,\dot{T},\zeta,\dot{\zeta}).$$

The superposition principle does not apply for the solutions of the non-linear differential equations. A formulation of the problem in complex notation is, for this reason, not necessarily of advantage. The main problem in the computation of the heat capacity of a system are the formulation of the Gibbs fundamental equations, Eq. (2), and the evaluation of a suitable expression for the coupling factor L. One can usually solve the determining differential equations numerically (in real notation) if $g(T,p,\zeta)$ and $L(T,p,\zeta)$ are known [36]. In the Section of Discussions on heat capacities in transition regions, we proceed from Eq. (3) with a Taylor expansion of the affinity a.

The heat flow in dissipative systems

The change of entropy with time, $\dot{s}$, is separated in dissipative systems into two parts:

$$\dot{s}=\frac{\mathrm{d}_e s}{\mathrm{d}t}+\frac{\mathrm{d}_i s}{\mathrm{d}t}$$

where $d_e s/dt$ is the amount of entropy exchanged by the system with the surroundings (entropy flux), and $d_i s/dt \geq 0$ is the entropy produced in the interior of the system (entropy production), both per time and mass unit (for example [13]). If the temperature T of the system is also in non-equilibrium equal to the temperature of the surroundings, T^* (which does not necessarily have to be the case, [15, 36]) then:

$$\frac{d_e s}{dt} = \frac{1}{T}\dot{q}, \tag{40}$$

where $\dot{q}$ is the heat exchanged by the system per time and mass unit (specific heat flux, *hf*). The entropy production of the system is given by [13]:

$$\frac{d_i s}{dt} = \frac{1}{T} a \dot{\zeta}. \tag{41}$$

From Eqs (4) and (18b) one can then see that at constant pressure:

$$\frac{d_i s}{dt} = \left(1 - \frac{\eta_{T,p}}{T\sigma_{T,p}}\right)\frac{\Delta c_p}{T}\dot{T}. \tag{42}$$

For the change of the entropy with time, one obtains from Eq. (13) with Eqs (5) and (15) at constant pressure that:

$$\dot{s} = \frac{c_{p,\zeta}}{T}\dot{T} + \sigma_{T,p}\dot{\zeta} \tag{43}$$

and with Eq. (18):

$$\dot{s} = \frac{1}{T}(c_{p,\zeta} + \Delta c_p)\dot{T} = \frac{c_p}{T}\dot{T}. \tag{44}$$

Using Eqs (44) and (42), one obtains:

$$\frac{d_e s}{dt} = \dot{s} - \frac{d_i s}{dt} = \frac{1}{T}\left(c_{p,\zeta} + \frac{\eta_{T,p}}{T\sigma_{T,p}}\Delta c_p\right)\dot{T}.$$

The heat flow is given according to Eq. (40) by:

$$\dot{q} = \left(c_{p,\zeta} + \frac{\eta_{T,p}}{T\sigma_{T,p}}\Delta c_p\right)\dot{T}, \tag{45}$$

or with Eq. (18a) by:

$$\dot{q} = \left[\left(1 - \frac{\eta_{T,p}}{T\sigma_{T,p}}\right)c_{p,\zeta} + \frac{\eta_{T,p}}{T\sigma_{T,p}}c_p\right]\dot{T}. \tag{46}$$

Equations (45) or (46) describe, in general, the heat exchange of a dissipative system with its surroundings. Specifically in internal equilibrium one finds for the heat exchange, because of $\eta_{T,p}=T\sigma_{T,p}$ and $c_p=c_p^e$:

$$\dot{q} = c_p^e \dot{T}. \tag{47}$$

For the heat flux in the arrested equilibrium it follows because $\Delta c_p=0$ that:

$$\dot{q} = c_{p,\zeta} \dot{T}. \tag{48}$$

In the form $\dot{u}=\dot{q}-p\dot{v}$, the first law of thermodynamics holds also in non-equilibrium of a homogeneous system of constant mass at rest that is not exposed to locally variable, external force fields (u, specific internal energy of the system, v, specific volume). At constant pressure one finds in non-equilibrium that:

$$\dot{q} = \dot{\eta} = c_{p,\zeta} \dot{T} + \eta_{T,p} \dot{\zeta}.$$

If one assumes erroneously in analogy to Eq. (44) that the heat flux be given by:

$$\dot{q}_E = c_p \dot{T}, \tag{49}$$

one finds:

$$\dot{q}_E - \dot{q} = T \frac{d_i s}{dt} \geq 0 \tag{50}$$

as difference between the erroneous heat flux $\dot{q}_E$ and the true heat flux $\dot{q}$. This difference depends according to Eq. (42) on the heating or cooling rate. The percentage deviation, in contrast, is independent of T. With Eqs (42) and (45) it follows from Eq. (50) that:

$$\frac{\dot{q}_E - \dot{q}}{\dot{q}} = \frac{(T\sigma_{T,p} - \eta_{T,p})\Delta c_p}{T\sigma_{T,p} c_{p,\zeta} + \eta_{T,p}\Delta c_p}. \tag{51}$$

The error disappears in the vicinity of the internal equilibrium (with $a=T\sigma_{T,p}-\eta_{T,p}\approx 0$) and the arrested equilibrium (with $\Delta c_p\approx 0$).

In case of a periodic perturbation, as given in Eq. (22), one must write $T\sigma_{1,p}=\eta_{1,p}$ because of the coefficients refer to the internal equilibrium. With Eq. (46) one finds then the complex heat flow:

$$q = c_p(\omega)\dot{T}. \tag{52}$$

With Eq. (1) one can also write for the complex heat capacity:

$$c_p(\omega) = |c_p(\omega)|e^{i\theta}, \quad \text{with} \tag{53a}$$

$$|c_p(\omega)| = \sqrt{c_p'^2 + c_p''^2} \text{ and } \tan\theta = -\frac{c_p''}{c_p'}. \quad (53b)$$

With Eqs (52) and (22b) one can write:

$$\dot{q} = i\omega\Delta T|c_p(\omega)|e^{i(\omega t+\theta)}. \quad (54)$$

The heat flux is phase shifted by $\theta<0$ relative to the temperature flux $\dot{T}$. In the limiting cases $\omega\tau^e_{T,p}<<1$ and $\omega\tau^e_{T,p}>>1, c_p'' \approx 0$ holds, and therefore $\theta\approx 0$. In between the two limiting cases, $|\theta|$ reaches a maximum that does not necessarily coincide with the maximum of c_p'' because of the denominator c_p' in $\tan\theta$.

Discussion of experimental TMDSC data

Measurement and data analysis by TMDSC

The input parameters in TMDSC are the modulation at the sample temperature (amplitude A_T), the frequency ω, and an underlying heating rate $\langle\dot{T}\rangle$[c]:

$$T_s = A_T i e^{-i(\omega t-\varepsilon)} \quad (55)$$

where ε is the phase lag of the sample temperature at steady state from the heater temperature (or a reference oscillation). The present discussion is based on the heat-flux calorimeter of TA Instruments, the MDSC™ 2920, which achieves the preset sample-temperature amplitude A_T by controlling the heater temperature with the signal of the sample thermocouple. Figure 2 shows typical heater and sample temperatures at the beginning of a TMDSC experiment as a function of time, and the appropriate equations describing this process [8]. At steady state, the frequencies of heater and sample calorimeter are identical. For the reference calorimeter, a similar expression can be written (temperature T_r, amplitude A_r, phase lag φ). The temperature difference between reference and sample, $T_r-T_s=\Delta T$, which is proportional to the heat flow, HF (which, in turn, is equal to $\dot{q}$ of Eqs (45) and (54)), is then given (with a further phase-shift of $\pi/2$, see also Eq. (22b)) by:

$$\Delta T = A_\Delta e^{-i(\omega t-\delta)} \quad (56)$$

where A_Δ is the amplitude and δ, the phase lag. Figure 3 illustrates with a Lissajous diagram the approach to steady state and the slow increase of heat capacity which causes an increase in amplitude A_Δ and phase lag δ [17], as will be discussed next.

[c] Using $\sin\theta+i\cos\theta=ie^{i\theta}$. The more common $\cos\theta+i\sin\theta=e^{i\theta}$ of Eq. (1) differs from Eq. (55) by a phase shift of $\pi/2$, necessary since the initial condition at time zero is $T_s=0$.

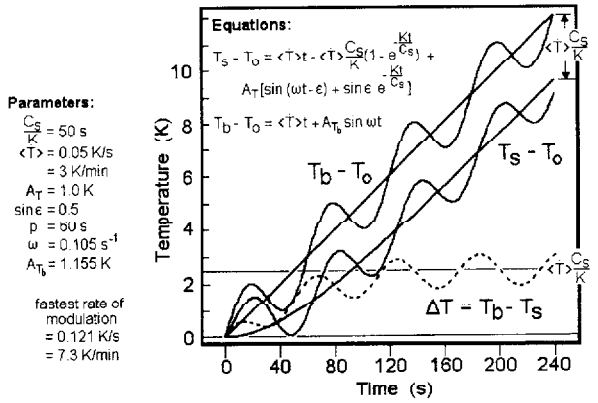

Fig. 2 Sample and heater (block) temperatures at the beginning of a TMDSC experiment [8]. The given equations are based on Newton's law of cooling $\dot{q}=K[T_b(t)-T_s(t)]$ [16]. The unmodulated temperatures represent a sliding average over one modulation period and, at steady state, are identical to the standard DSC temperatures

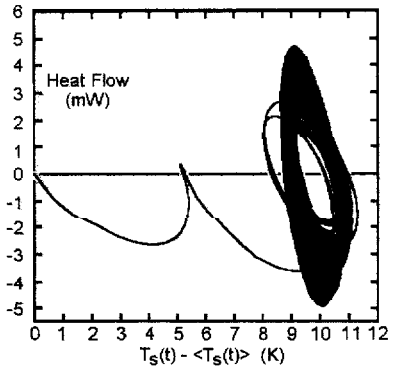

Fig. 3 Lissajous figure of a TMDSC experiment [17], showing the initial approach to steady state and the slow increase of heat capacity causing an increase in A_Δ and δ. Sample mass m: 61 mg; heating rate$\langle\dot{T}\rangle$: 5 K min^{-1}; mod. period: 80 s; mod. amplitude A: 1.0 K

At steady state Eqs (55) and (56) can be inserted into the equation for the temperature difference, which eliminates the heater temperature, T_b, from consideration if the two calorimeters are identical, i.e. have the same Newton's law constant K [16]:

$$T_r - T_s = \frac{C_s - C_r}{K}\frac{dT_s}{dt} - \frac{C_r}{K}\frac{d(T_r - T_s)}{dt} \quad (57)$$

The heat capacities for sample and reference calorimeters (contents and pans) are C_s and C_r, respectively, and are assumed constant over at least one modulation

period. From the solution of Eq. (57) expressions for the heat capacity difference and phase angles can be derived [9]:

$$|C_s - C_r| = \frac{A_\Delta}{A_T}\sqrt{(K/\omega)^2 + C_r^2} \tag{58}$$

$$C_s = \frac{K}{\omega}\tan c. \tag{59}$$

Since C_r is usually an empty calorimeter of heat capacity C', only the positive answer of Eq. (59) is of interest. Using a reference calorimeter identical to the empty sample calorimeter, Eq. (58) gives a simple expression for the specific heat capacity c_p of a sample of mass m:

$$mc_p = \frac{A_\Delta}{A_T}\sqrt{(K/\omega)^2 + C'^2}. \tag{60}$$

After correction for remaining asymmetry of sample and reference calorimeters [18], calibration with sapphire, which has a well-known heat capacity [19], permits to eliminate the expression under the square root for measurements under identical conditions.

For data analysis, the resulting heat flow in TMDSC can be expressed as a Fourier series:

$$HF(t) = b_0 + \sum_{\nu=1}^{\nu=\infty}\left[a_\nu \sin\frac{2\pi\nu}{p}t + b_\nu \cos\frac{2\pi\nu}{p}t\right], \tag{61}$$

with the constant b_0 and the amplitudes a_ν and b_ν, given by:

$$b_0 = \frac{1}{p}\int_{-p/2}^{+p/2} HF(t)\mathrm{d}t \tag{62}$$

$$a_\nu = \frac{2}{p}\int_{-p/2}^{+p/2} HF(t)\sin\left(\frac{2\pi\nu}{p}t\right)\mathrm{d}t \tag{63}$$

$$b_\nu = \frac{2}{p}\int_{-p/2}^{+p/2} HF(t)\cos\left(\frac{2\pi\nu}{p}t\right)\mathrm{d}t, \tag{64}$$

where ν is a running integer, starting from 1, and p is the modulation period in s.

The data evaluation starts with b_0, which is the total heat flow $<HF(t)>$. The integration in Eq. (62) is replaced by a sum. Assuming a typical p of 100 s and steps of 2 s, one gets:

$$<HF(t)> = \frac{\sum_{t-50}^{t+50} HF(t) - \frac{1}{2}HF(t-50) - \frac{1}{2}HF(t+50)}{50} \quad (65)$$

For a sinusoidal modulation of frequencies $\nu\times\omega$ and constant or linearly increasing heat flow over one modulation period, the total heat flow is, thus, the same as would have been measured by standard DSC without modulation.

Next, one realizes that one can conveniently rewrite the Fourier series of Eq. (61) in terms of $HF_{(corr)}=HF(t)-<HF(t)>$. This transforms the data into a pseudo-isothermal analysis. It includes b_0, which accounts for the effect of $<\dot{T}>$, in the left-hand side of Eq. (61). This analysis is also identical to the quasi-isothermal experiment of AC calorimetry [20] which operates with $<\dot{T}>=0$. Wider temperature ranges in quasi-isothermal experimentation are covered with a series of runs with step-wise increases in temperature [21].

One can, furthermore, recognize that for a strictly sinusoidal response with frequency ω, only terms with a_1 and b_1 in the Fourier series need be considered. As before, the integrations of b_1 and a_1, as expressed in Eqs (63) and (64), are calculated by averaging over the full period, p. The Fourier coefficients can then be written in the TMDSC nomenclature as $a_1=2<HF_{sin}(t)>=A_{HF}\cos\delta$ and $b_1=2<HF_{cos}(t)>=A_{HF}\sin\delta$, with:

$$<HF_{sin}(t)> = \frac{\sum_{t-50}^{t+50} HF_{sin}(t) - \frac{1}{2}HF_{sin}(t-50) - \frac{1}{2}HF_{sin}(t+50)}{50}, \text{ and} \quad (66)$$

$$<HF_{cos}(t)> = \frac{\sum_{t-50}^{t+50} HF_{cos}(t) - \frac{1}{2}HF_{cos}(t-50) - \frac{1}{2}HF_{cos}(t+50)}{50}. \quad (67)$$

The amplitude of heat flow is then:

$$A_{HF} = 2\sqrt{<HF_{sin}(t)>^2 + <HF_{cos}(t)>^2}. \quad (68)$$

Using the TA Instruments software, the output of the data analysis is further smoothed by computing an additional average before insertion into Eq. (60):

$$<A_{HF}(t)>_{smoothed} = \frac{\sum_{t-50}^{t+50} A_{HF}(t) - \frac{1}{2}A_{HF}(t-50) - \frac{1}{2}A_{HF}(t+50)}{50} \quad (69)$$

The pseudo-isothermal as well as quasi-isothermal data analyses give thus the first harmonic of the heat flow of frequency ω, and care must be taken in interpreting data if higher harmonics and components of other frequencies are contained in the heat flow response. Analogous calculations are done for the amplitude of the measured sample temperature for insertion into Eq. (60).

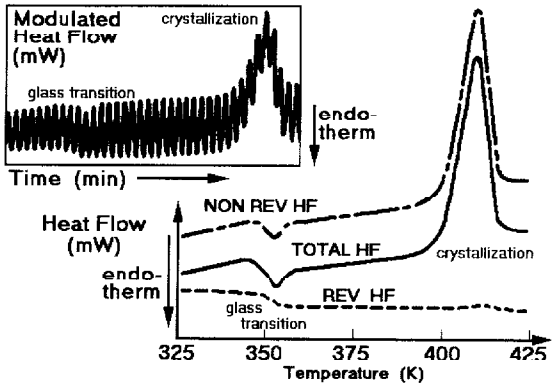

Fig. 4 Amorphous PET analyzed by TMDSC [22] (pseudo-isothermal data analysis). $\langle T \rangle$: 5 K min^{-1}; p: 30 s; A_T: 0.6 K; sample: 4.5 mg

Figure 4 copies part of the first TMDSC analysis of a quenched poly(ethylene terephthalate), PET [22]. The insert shows $HF(t)$, the main TMDSC-curves, the reversing heat flow (Eq. (69)], the total heat flow (Eq. (65)), and the nonreversing heat flow. The latter is the computed difference between total and reversing heat flows. The enthalpy relaxation is visible only in the total and nonreversing heat flows. Similarly, the cold crystallization at about 410 K does not af-

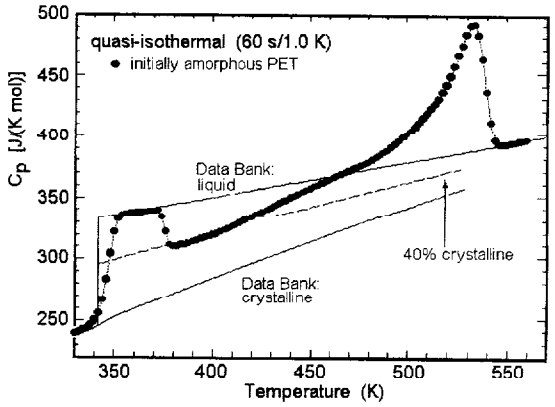

Fig. 5 Heat capacity of a similar sample as shown in Fig. 4, analyzed quasi-isothermally [24]. The thin lines represent comparisons with data bank heat capacities derived from adiabatic calorimetry and standard DSC, as well as computed data for the crystallinity of the sample after cold crystallization

fect the reversing heat flow. Model calculations show that exponential additions to a modulated heat flow have practically no component in the reversing signal, while abrupt jumps or sharp peaks contribute their, often small, Fourier component of frequency ω [23].

Figure 5 shows a typical quasi-isothermal experiment with a similar amorphous PET as in Fig. 4 [24]. The data were derived using Eq. (60). The heat capacities of the solid (glassy, up to about 330 K), the supercooled liquid (355–370 K), and the liquid (>550 K) agree well with the data by adiabatic calorimetry and DSC, also shown in the figure by the thin lines. The changes in the glass transition, on cold crystallization, and the broad melting region need special attention.

Heat capacity of solids and liquids

The reversing heat capacities calculated from Eq. (60) in the solid and liquid states are shown in Fig. 5 to agree with classical calorimetry. This is expected from the fast response of molecular motion relative to macroscopic changes in temperature, as documented in the Introduction. With the fast relaxation times in the liquid, and the arrested equilibrium in the glassy solid, the dissipative parts of the complex heat capacity approach zero, as expressed in Eqs (33a) and (33b), respectively. The phase angles ε and δ of Eqs (55) and (56) are in both cases due to the limited thermal conductivity of the calorimeters. Only in the transition regions may the sample response be slow, and thus the introduction of a complex heat capacity with a non-zero dissipative part $c_p''(\omega)$ may be useful (Eqs (27) to (31)). The fact that in solids and liquids there is no dissipative contribution to the complex heat capacity causes $c_p(\omega) \approx c_p(\omega)'$ and has been made use of for the calibration of TMDSC by setting the baseline for the evaluation of a phase angle θ for complex heat capacity, as defined in Eq. (1).

The heat capacities in the solid states (glassy and crystalline) above about 50 K are practically independent of the value of the internal variable ζ and correspond closely to their vibrational contributions. This can be taken as the basis to set $c_{p,\zeta} \approx c_{p,\zeta}^e$ in Eq. (15). With the liquid heat capacity being c_p^e, one can, next, approximate the extrapolated difference between liquid and solid heat capacity as $\Delta^e c_p$ (Eq. (16a)).

Heat capacities in transition regions

More quantitative TMDSC at different frequencies and amplitudes of the glass transition of polystyrene [25] and PET [26] revealed that, indeed, it seems possible to separate the hysteresis effects as shown in Fig. 4 and, in addition, evaluate the frequency-dependence of the heat capacity in the glass transition region. Figure 6 shows plots of the Lissajous figures in the glass transition region of amorphous PET as also shown in Fig. 5. The superposition of 10 modulation

cycles indicates steady state. Analysis of the data is, however, difficult because of the large distance from equilibrium which leads to a changing L, as pointed out the Section on Limits of the linear response theory. Equation (39) shows that the effective relaxation time measured at constant pressure is dependent on the rate of change of T and ζ, in addition to L being a function of T and ζ itself.

Analysis of the reversing heat capacity was made in real notation making using the 'hole model' [7, 11]. The number of holes ζ is then the internal variable. The hole model allows the calculation of the kinetics of the change of ζ as a function of time at constant pressure:

$$\frac{d\zeta}{dt} = \frac{1}{\tau}(\zeta^e - \zeta) \tag{70}$$

with τ representing a relaxation time linked to an activation energy of hole formation derived from the time-dependence of the liquid heat capacity. For T, p, L=constant and $\tau \approx \tau^e_{T,p}$, Eq. (70) can be linked to the irreversible thermodynamics (Eq. (19)). These conditions are, however, not fulfilled for the glass transition. Equation (70) has, thus, been solved numerically for typical TMDSC parameters using an Arrhenius expression [27], and also, with similar results, using a single-parameter version of the KAHR model commonly applied to analyze DMA data on the glass transition [28].

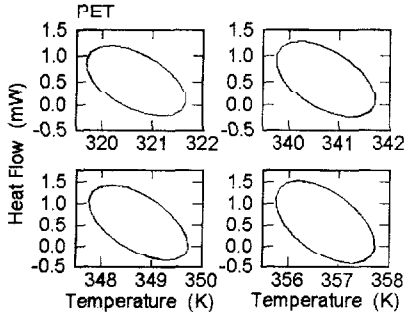

Fig. 6 Lissajous figures in the glass transition region of PET for quasi-isothermal analyses. Each run was of 20 min, of which the last 10 min were analyzed. Quasi-isothermal p: 60 s; A_T: 1.0 K; sample: ≈5 mg

With the hole model one can solve the non-linear Eq. (70) numerically and find ζ as a function of time and temperature on cooling, as shown in Fig. 7 for PET [27]. The initial number of holes is the equilibrium value at T_0, the starting temperature, ζ^e. The decrease in number of holes and the decrease in oscillation amplitude in the glass transition is clearly shown.

With hole energies and equilibrium numbers of holes calculated from the heat capacities of the liquid and glass, the total and reversing apparent heat capacities in the glass transition region can be calculated, as shown in Fig. 8. The calcula-

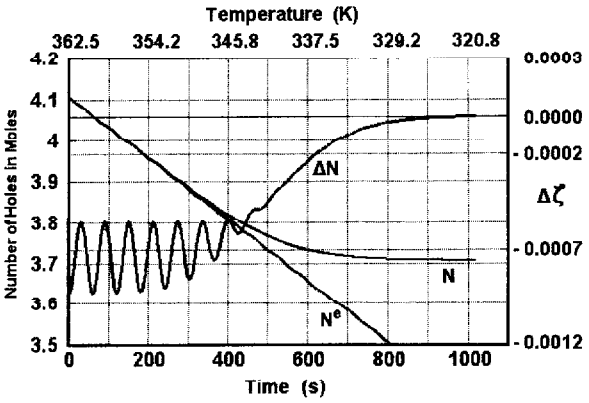

Fig. 7 Calculation of the freezing of the hole equilibrium of PET. $\langle \dot{T} \rangle$: –2.5 K min^{-1}; A_T: 0.1 K; p: 60 s, time: 0–1020 s=362.5–320 K

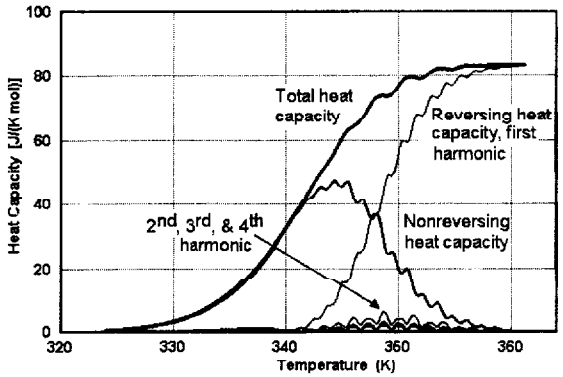

Fig. 8 Calculation of the total, reversing, higher harmonics, and non-reversing heat capacities, using numerical solutions of Eq. (70)

tions were done as in the TA Instruments software, indicated by Eqs (66)–(68), leaving out the last smoothing step of Eq. (69) to better assess smaller effects. The remaining oscillations in the total heat capacity could be linked to the interference of the underlying heating rate with the modulation, which leads to a small change in oscillation frequency (Doppler effect). The reversing heat capacity is the first harmonic, as computed from Eq. (60). It could be shown by partial solution of the heat-flow equations that small, but not negligible contributions come from the second harmonic, not evaluated by Eqs (66)–(68) [12]. This contribution is due to the exponential change of relaxation time which gives on modulation a larger effect on heating than on cooling. Finally, there is for the same reason also a constant increase of the base-line of the oscillating heat flow. This contribution is, naturally, also included in the total heat capacity b_0. Figure 8 shows, furthermore, the third and fourth harmonic contributions which are

mainly due to the change in modulation frequency. Overall, it seems thus that the glass transition can be studied by TMDSC, but it is necessary to develop more transparent software for the detailed analysis of the kinetics. One needs to know to what degree the temperature control may compensate the frequency shift and have a more detailed temperature profile within the sample. It may not be enough to assume a negligible temperature gradient within the sample. All these special effects are, however, small, and until recently were smaller than the error limit.

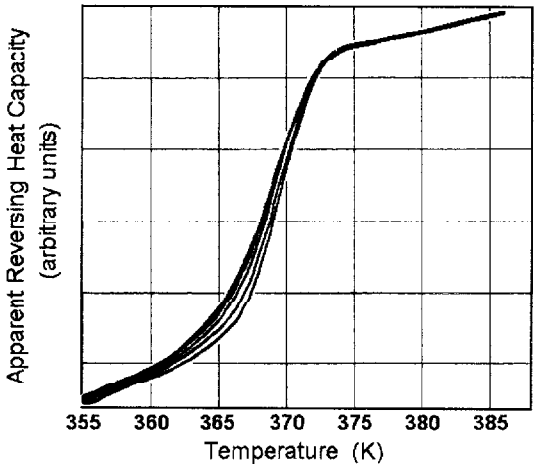

Fig. 9 Apparent reversing heat capacities of polystyrenes of different thermal histories under identical heating and modulation conditions [25]. Run on heating after annealing left to right: at 373 K for 30 min; at 369 K for 30 min; at 366.6 K for 30 min; at 363 K for 60 min; at 360.5 K for 180 min; at 358 K for 240 min. (sample: 5.9 mg, heating rate: 2 K min^{-1}; p: 80 s; A_T: 1.K)

Additional observations on the TMDSC in the glass transition point to needed improvements in the description of the kinetics. The relaxation time in Eq. (70) is dependent on the internal variable through a cooperative effect [7]. Figure 9 illustrates the standard reversing heat capacity in the glass transition region measured on a series of differently annealed polystyrenes by heating under identical conditions [25]. Although the changes in the reversing heat capacity are not large, they are easily measurable and correlate with the size of the hysteresis effect in the nonreversing contributions. A second indication of cooperativity arises when comparing the glass transition on heating and cooling with the quasi-isothermal measurements.

Figure 10 shows a typical example. Close to the liquid state, the separation of the reversing heat capacity on heating and cooling from the quasi-isothermal data can be duplicated by solving Eq. (70). The cross-over on approaching the glass cannot be explained in this fashion, but needs to include cooperative terms [29]. Again, the effects are small, but clearly measurable. Introduction of a com-

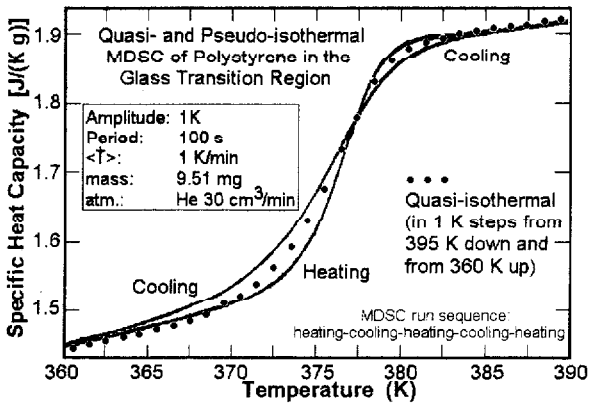

Fig. 10 Experimental reversing heat capacity of polystyrene in the glass transition region on TMDSC and quasi-isothermal analysis [29]. (Three heating runs, two cooling runs, and two sets of quasi-isothermal runs are superimposed, the quasi-isothermal runs were done step-wise, once on heating, once on cooling.)

plex heat capacity for the analyses of these phenomena seems of little advantage, particularly since linear response is lost close to the eqilibrium of the liquid state.

The TMDSC in temperature ranges of absorption or evolution of latent heats is of particular interest. The early discovery of the practically complete exclusion of irreversible, exponential processes from the reversing heat capacity, as illustrated by the cold crystallization of PET in Fig. 4, is a typical example. Under such circumstances the reversing heat capacity can be measured with good precision in the presence of rather large heat effects. Care must be taken, however, that the latent heat effects do not disturb the steady state of the modulated portion of the heat flow and that the non-modulated latent-heat effect does not have any components in the Fourier series of Eq. (61). Besides the crystallization shown in Fig. 4, evaporation, sublimation, and chemical reactions (such as oxidation, pyrolysis, and curing) are examples that otherwise make heat capacity measurements by standard DSC impossible. The heat capacity measured under these conditions needs to be analyzed as described in the Section on Heat capacities of solids and liquids after it has been ascertained that the latent heat effect on the reversing heat capacity is negligible. As long as the measured substance is liquid or solid, the dissipative contribution to the complex heat capacity should be negligible. In case the heat capacities changes due to the change of state, the kinetics of the reaction can be followed by TMDSC. A specially successful example has been the detection of the changes of the glass transition temperature during curing of thermosetting polymers [30].

The case of a sharp equilibrium transition is illustrated in Fig. 11. The figure represents plots of the sample (sensor) temperature and the heat flow $HF(t)$ [31]. Clearly, enormous melting peaks are added to the relatively small modulated

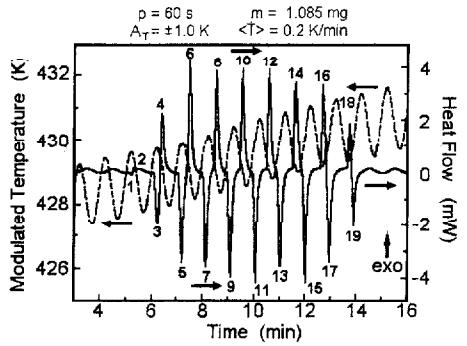

Fig. 11 Time-domain recording of the TMDSC of melting range of indium as an example of sharp, reversible melting [31]. Even numbers in the graph refer to crystallization, odd ones to melting. Peaks 5 to 15 agree with the heat of fusion of indium 28.6 J g^{-1}. Dashed line: temperature of sensor of sample. Solid line: heat flow $HF(t)$

heat flow due to heat capacity (seen below 5 and above 14 s). As indicated in the figure, after the first few melting and crystallization peaks almost full melting and crystallization is possible during each cycle. The quantitative analysis of this trace can only be done in the time domain, i.e. analogous to standard DSC with a wavy baseline. One must assume that the sample temperature is constant between the beginning and peak of melting (at the equilibrium melting temperature T_m) [16]. The sensor temperature is, however, driven to higher temperature by the heat flow required by the modulation program that attempts to reach amplitude A_T. A modulation of the reference temperature would not change the modulation of the heater temperature and record a more constant sample temperature. A trace as in Fig. 11 is useful for calibration of the TMDSC. Of interest is also the retention of nuclei that avoids supercooling in the immediate vicinity of the melting temperature and permits calibration of the heating as well as cooling cycle. For

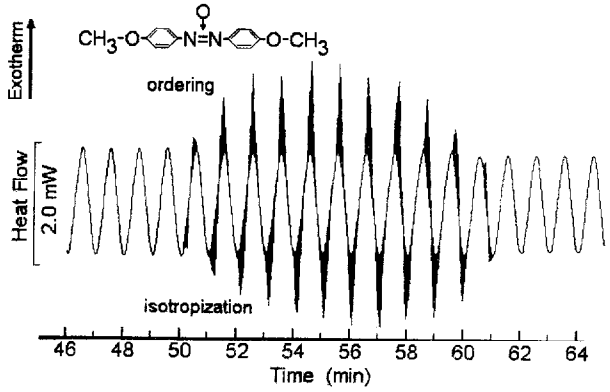

Fig. 12 Time-domain recording of the TMDSC of isotropization of a liquid crystal as an example of a reversible, slightly broader transition [32]. Mettler-Toledo TMDSC <$\dot{T}$>: 0.1 K^{-1}; A_T: 1.0 K; p: 60 s; sample: 5.92 mg

indium, the melting and crystallization rates are sufficiently fast that there seems little chance to study time effects at the transition. An example of the reversible isotropization and ordering of a liquid crystal is shown in Figure 12 [33]. In this case the change in heat-flow is only a factor of about two and a heat flow without transition is drawn in the transition range, using information from outside the transition region. Again, it can be seen that steady state is lost and the analysis must be carried out as in standard DSC.

Extracting the reversing heat flow from experiments as given in Figs 11 or 12, as outlined in Eqs (65)–(69), would give the first harmonic of the Fourier series that matches simultaneously the heat capacity and latent heat components of the heat-flow response. Although one expects a larger value for Eq. (69), its magnitude can not be linked directly to the reversible heat of transition and computation of a complex heat capacity is of little additional value.

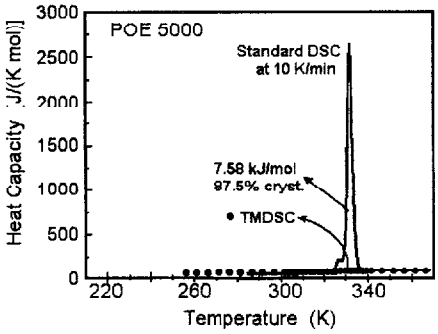

Fig. 13 Comparison of standard DSC and quasi-isothermal TMDSC of poly(oxyethylene) of molar mass (5000) [34]. Quasi-isothermal p: 60 s; A_T: 0.5 K; sample mass: 1.0 mg; RCS cooling

Turning to the melting transition of polymers, it is well known that such materials do not have a melting/crystallization equilibrium [33]. The irreversible nature is illustrated in Fig. 13 on the example of a well-crystallized poly(oxyethylene), POE. The quasi-isothermal TMDSC shows practically no effect of melting, while the standard DSC indicates the melting peak [34].

The broad melting range that is common for many macromolecules may be analyzed in the same fashion as shown in Fig. 13 with the assurance that well grown polymer crystals do not contribute to the reversing heat capacity of quasi-isothermal TMDSC. The quasi-isothermal mode is preferred in these experiments in order to assure the attainment of steady state after the initial increase of temperature which causes the corresponding irreversible melting.

A surprising result is, however, the curve of Fig. 5. It shows a rather broad increase in the reversing heat capacity in the melting range. The maximum level attained is lower than found in a standard DSC trace which reveals the full heat of fusion (peak height about 900 J K^{-1} mol^{-1}). Less than 10% of the heat of fusion is found underneath the endothermic, reversing heat capacity. A detailed analysis

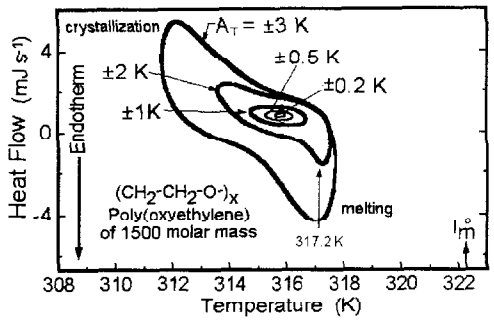

Fig. 14 Lissajous figures of the melting and crystallization of a low molecular mass poly(ethylene oxide) (1500) with different modulation amplitudes showing a region of metastable melt between crystallization and melting temperatures [34]

suggests that a local melting/crystallization exists on a molecular basis in these poorly crystallized materials [24]. This local equilibrium changes with time and the reversing heat capacity drifts over many hours towards the expected heat capacity level of the semicrystalline material, but seemingly without ever reaching it [35]. Additional observations were made on lower molar mass polymers, shown in Fig. 14 [34]. In this case the range of metastability of the polymer melt could be bridged for a small fraction of the polymer by temperature modulation with a sufficiently large amplitude. The Lissajous figures reveal the well-separated crystallization and melting domains. Again, the long-time experiment indicate that the produced crystal fractions are not constant with time. In this case they increase with time, probably due to diffusion limited access to crystallization sites.

These experiments with TMDSC in regions of latent heat evolution and absorption show a rich field of study of irreversible effects that has barely been touched. The examples indicate that as soon as larger amounts of latent heat are involved, great care must be taken to assess the steady state and determine the limits of sample mass and modulation parameters for quantitative experiments. In most cases the analysis of heats of transition are best done in the time domain. For reversible heats of transition, the heat flow is usually not sinusoidal, leading to limited information with analyses using the first harmonic only. In case the heat capacity of the material in the transition region can be assessed, the same methods as described above can be used. The use of a complex heat capacity seems limited in most cases, although one can imagine that transitions with low latent heats and a suitable transition rate may fall into the range of validity established in the Section on the Limits of the linear response theory.

Conclusions

The development of TMDSC has opened the door to many investigations not possible with standard DSC. The use of complex heat capacity in analogy to

DME and DETA measurements is more complicated because of the change of the enthalpy and entropy with the change in temperature, not present in the latter two analysis methods. Furthermore, over wide ranges of temperature the dissipative contribution approaches zero. The major application to date seems the glass transition. In this case the complex heat capacity is however non-linear. Up to now the application of complex heat capacity in TMDSC has been of limited use and may, if applied in non-linear situation, be the cause of serious error.

* * *

This work was supported by the Division of Materials Research, National Science Foundation, Polymers Program, Grant # DMR 97-03692 and the Division of Materials Sciences, Office of Basic Energy Sciences, U. S. Department of Energy at Oak Ridge National Laboratory, managed by Lockheed Martin Energy Research Corp. for the U. S. Department of Energy, under contract number DE-AC05-96OR22464.

References

1 see, for example R. Kubo, M. Toda and N. Hashitsume, 'Statistical Physics II', Springer, Berlin, 1985.
2 see, for example, Schawe, J. E. K., Thermochim. Acta, 261 (1995) 183.
3 M. Reading, Trends in Polymer Sci., 8 (1993) 248.
4 B. G. Sumpter, D. W. Noid, G. L. Liang and B. Wunderlich, Adv. Polymer Sci., 116 (1994) 27.
5 M. Reading, D. Elliot and V. L. Hill, J. Thermal Anal., 40 (1993) 949; P. S. Gill, S. R. Sauerbrunn and M. Reading, ibid., 931.
6 B. Wunderlich, 'Thermal Analysis', Academic Press, Boston, 1990.
7 B. Wunderlich, D. M. Bodily and M. H. Kaplan, J. Appl. Phys., 35 (1964) 95.
8 B. Wunderlich, A. Boller, I. Okazaki and S. Kreitmeier, Thermochim. Acta, 282/283 (1996) 143.
9 B. Wunderlich, Y. Jin and A. Boller, Thermochim. Acta, 238 (1994) 277.
10 see, for example F. O. Rice, Phys. Rev., 31 (1928) 691; or J. O. Hirschfelder, C. F. Curtis, and R. B. Bird, 'Molecular Theory of Gases and Liquids', J. Wiley and Sons, New York, 1954.
11 N. Hirai and H. Eyring, J. Appl. Phys., 29 (1958) 810; J. Polymer Sci., 37 (1959) 51.
12 B. Wunderlich, A. Boller, I. Okazaki and S. Kreitmeier, J. Thermal Anal., 47 (1996) 1013.
13 I. Prigogine, 'Introduction to Thermodynamics of Irreversible Processes', Interscience, New York, 1961.
14 E. A. Guggenheim. 'Thermodynamics.' North-Holland Publ. Co., Amsterdam, 1959.
15 J. Meixner, Z. Physik, 219 (1969) 79.
16 B. Wunderlich, 'Thermal Analysis', Academic Press, Boston, 1990.
17 M. Varma-Nair and B. Wunderlich, J. Thermal Anal., 46 (1996) 879.
18 A. Boller, I. Okazaki, K. Ishikiriyama, G. Zhang, and B. Wunderlich, J. Thermal Anal., 49 (1997) 1081.

19 D. A. Ditmars, S. Ishihara, S. S. Chang, G. Bernstein and E. D. West, J. Res. Natl. Bur. Stand., 87 (1982) 159.
20 P. F. Sullivan and G. Seidel, Phys. Letters, 25(A) (1967) 229; Phys. Rev., 173 (1968) 679.
21 A. Boller, Y. Jin and B. Wunderlich, J. Thermal Anal., 42 (1994) 307.
22 M. Reading, B. Hahn and B. S. Crowe, US Patent 5.224.775 (July 6, 1993).
23 B. Wunderlich, J. Thermal Anal., 48 (1997) 207.
24 I. Okazaki and B. Wunderlich, Macromolecules, 30 (1997) 1758.
25 A. Boller, C. Schick and B. Wunderlich, Thermochim. Acta, 266 (1995) 97.
26 I. Okazaki and B. Wunderlich, J. Polymer Sci., Part B: Polymer Phys., 34 (1996) 2941.
27 B. Wunderlich and I. Okazaki, J. Thermal Anal., 49 (1997) 57.
28 J. M. Hutchinson and S. Montserrat, Thermochim. Acta, 286 (1996) 263.
29 L. C. Thomas, I. Okazaki and B. Wunderlich, Thermochim. Acta, 291 (1997) 85.
30 G. Van Assche, A. Van Hemelrijck, H. Rahier and B. Van Mele, Thermochim. Acta, 268 (1995) 121; 286 (1996) 209.
31 K. Ishikiriyama, A. Boller, and B. Wunderlich, J. Thermal Anal., 50 (1997) 547.
32 W. Chen and B. Wunderlich, Proc. 25th NATAS Conf. in McLean, Va., Sept. 7–9. 1997, R. G. Morgan, ed., 637; Thermochim. Acta., submitted for publication in (1998).
33 B. Wunderlich, 'Macromolecular Physics, Vol. III, Crystal Melting', Academic Press, New York, 1980.
34 K. Ishikiriyama and B. Wunderlich, Macromolecules, 30 (1997) 4126; J. Polymer Sci., Part B. Polymer Phys., 35 (1997) 1877.
35 I. Okazaki and B. Wunderlich, Macromol. Chem. Phys. Rapid Comm., 18 (1997) 313.
36 H. Baur, Z. Naturforschung, 53A (1998) 157.